ACS OMEGA

Open Access

http://pubs.acs.org/journal/acsodf

Article

A Novel Poly(cytosine)-Based Electrochemical Biosensor for Sensitive and Selective Determination of Guanine in Biological Samples

Melaku Metto,* Alemu Tesfaye, Minaleshewa Atlabachew, Atakilt Abebe, Tihunie Fentahun, and Abaineh Munshea

Cite This: *ACS Omega* 2024, 9, 26222−26234

Read Online

ACCESS | Metrics & More | Article Recommendations | Supporting Information

ABSTRACT: The novel poly(cytosine)-modified glassy carbon electrode-based electrochemical sensor was fabricated potentiodynamically for the detection of Guanine (G) in clinical and biological samples. The surface of the electrode was successfully activated by electropolymerization, and about a 7.5-fold current improvement due to modification was achieved. From the analysis of the dependence of peak current and peak potential on a scan rate, a higher R^2 for the peak current on the square root of scan rate (R^2 = 0.999) than the dependence of peak current on scan rate (R^2 = 0.982) indicated that the oxidation of G at poly(cytosine)/GCE was predominantly diffusion controlled. The oxidative peak response of the electrode revealed a high linear range of G concentration (0.1−200 μM) under optimized conditions. The detection limit and limit of quantification were 6.10 and 20.13 nM, respectively, associated with the %RSD of under 1%. The validation of the developed electrochemical sensor for the determination of G was investigated by analyzing human urine DNA and serum samples with spike recovery results in the range of 98.20−103.70% with the interferent recovery percentage in the range of 97.86−103.10% containing 50−300% of potential interferents. The newly designed sensor demonstrated the highest level of performance for the G detection in real samples.

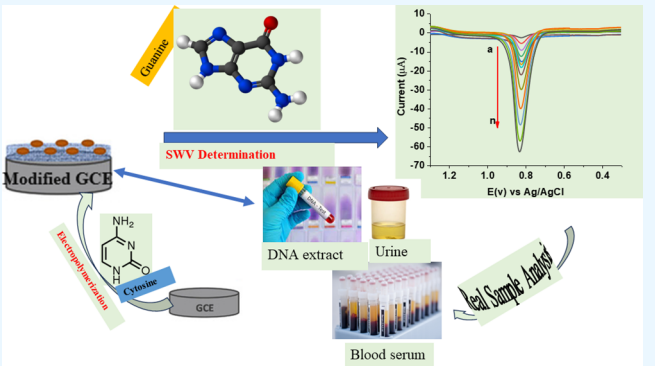

1. INTRODUCTION

Healthy growth and development in the human body depend heavily on biomolecules like guanine, which are essential nucleic bases found in deoxyribonucleic acid (DNA) and ribonucleic acid (RNA) molecules.[1] These biomolecules such as proteins are physiologically important materials that cover highly abundant constituents for the human body next to water.[2] Guanine (G) is one of the most important oxypurine organic bases that is involved in building both DNA and RNA. It plays several roles in biological systems in processes like energy supply, coenzyme formation, and metabolic regulation.[3] It is highly regarded as an important material in regulating coronary and cerebral circulation, releasing neurotransmitters, controlling blood flow, preventing arrhythmias, and modulating the activity of adenylate cyclase.[2] Its abnormal concentration variation in the biological systems is associated with an indication of mutation of the immune system and various diseases, including acquired immune deficiency syndrome (AIDS), epilepsy, mental retardation, cancer, and tumorigenesis.[1,4−6] Thus, the development of innovative biosensors that enable the identification and measurement of particular molecules facilitates the detection and surveillance of illnesses such as cancer and AIDS.

In this regard, many analytical methods, such as chemiluminescence,[7] gas chromatography,[8] high-performance liquid chromatography,[9] and micellar electrokinetic chromatography with indirect laser-induced fluorescence detection,[10] have been employed in determining G from different samples. Even though most of these reported methods may have high advantages such as ease of operation, high sensitivity, user-friendliness, and assay selectivity, they may have one or more of the drawbacks of either being expensive, time-consuming, requiring tedious sample preparation procedures, or needing skilled manpower. There is still a need for reliable and simple methods.[11,12] The electrochemical methods simplify the mentioned drawbacks owing to their simplicity, rapid response, and low cost, offering a greater sensitivity and dynamic range comparable to other analytical methods.[11,13,14]

Received: February 28, 2024
Revised: May 16, 2024
Accepted: May 30, 2024
Published: June 6, 2024

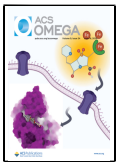

Furthermore, electroanalytical biosensors have been employed to determine G directly from blood samples using bare electrodes.[15] However, because of the limited surface area of the electroactive parts and low electron transfer, the response for the direct oxidation of G has been very poor on bare electrodes.[16] To eradicate limitations, such as difficulties, enormous chemically modified electrodes by utilizing different materials, such as nanomaterials,[17,18] and graphene,[19] resulting in more electrochemical active sites, have been fabricated and revealed improved oxidation signals. Nevertheless, almost all of them employed complicated and time-consuming procedures of electrode preparation, showed very short linear range, large background current, easy leakage of the surface-immobilized materials, and low catalytic activities.[18] Therefore, there is still a need for novel, improved, simple, and stable electrodes modified chemically through different materials with high selectivity and greater sensitivity to investigate G from different matrices.

Hence, developing a more accurate, selective, faster, low-cost, and sensitive method for the qualitative detection and quantitative determination of G is crucial. In this regard, cytosine (C) could be used as an electrode modifier for biosensing G from different clinical and biological samples.

Cytosine (C) is an aminopyrimidine nucleobase contained in RNA and DNA along with uracil/thymine, adenine, and G. Little or no reports could be found regarding the utilization of polycytosine as a modifying substrate for glassy carbon electrodes. Hence, this work demonstrates the fabrication, characterization, and application of a novel electrochemical biosensor based on poly(cytosine)/GCE for the determination of G in blood serum, human urine, and blood DNA extract samples using voltammetry, especially the square wave voltammetric method.

2. EXPERIMENTAL PART

2.1. Chemicals and Apparatus. Analytical grades of guanine and cytosine standards (99.0%, Sigma-Aldrich) were obtained from Ethiopian food and drug administration (EFDA), analytical grade of potassium hexacyanoferrate a standard couple of $K_3[Fe(CN)_6]$ and $K_4[Fe(CN)_6]$ (98.0%, BDH laboratories supplies, England), K_2HPO_4 and KH_2PO_4 (98%, Blulux laboratories (P)Ltd.), highly pure KCl (99.5%, from Blulux laboratories (p) Ltd.), NaOH (Extra pure, Lab Tech Chemicals), sodium acetate (99.7%, Blulux laboratories (p) Ltd.), and HCl (37%, Fisher Scientific), acetic acid (Fisher Scientific), sulfuric acid (loba Chemie), boric acid (from Blulux laboratories (p) Ltd.), and orthophosphoric acid (loba Chemie) were among the chemicals used. A 0.50 M H_2SO_4 stock solution was used for stabilizing the bare and modified electrodes. The buffer solutions, such as phosphate buffer solutions (PBS), acetate buffer solutions (ABS), and Britton-Robinson buffer solutions, were prepared from their respective acids and conjugate bases in deionized water, and the pH was adjusted using 1.0 M NaOH and 0.1 M HCl solutions. Instruments such as pH meter (AD8000, Romania), refrigerator (Lec. refrigeration PLC, England), CHI 760E potentiostat (Austin, Texas, USA), deionizer (Evoqua water technologies), and electronic balance (Nimbus, ADAM equipment, USA) were also among the instruments/apparatus used.

2.2. Analytical Procedure. *2.2.1. Solution Preparation.* The stock standard solution of 5 mM G was prepared in a 50 mL graduated flask by dissolving 37.78 mg of G powder in deionized water. The working solution of different concentrations of G in a 0.1 M appropriate buffer solution of optimum pH was prepared from the stock solution by serial dilution. A 1 mM cytosine monomer was prepared by dissolving an exact 4.50 mg of cytosine powder with deionized water in a 25 mL flask.

2.2.2. Electrochemical Measurements. An electrochemical cell contained with a three-electrode system composed of a bare glassy carbon electrode, GCE (3 mm diameter, PEEK GCE Glassy Carbon Electrode), or poly(cytosine)/GCE as a working electrode, silver/silver chloride (3.0 M KCl) as a reference electrode, and platinum coil electrode as a counter was employed for all electrochemical measurements of the target solution. Meanwhile, cyclic voltammetry (CV) and electrochemical impedance spectroscopy (EIS) were used for the characterization of electrochemical behavior and the surface catalysis of the bare and modified electrodes using $Fe(CN)_6^{3-/4-}$ as a probe, and the CV was applied for the electrochemical qualitative investigation of G. The square wave voltammetric technique was used for the quantitative determination of G and to validate the electrochemical performance of the developed biosensor.

2.2.3. Fabrication of Electrode. First, a bare (unmodified) glassy carbon electrode was polished to a mirror-like finish surface with alumina slurries on a polishing cloth and then continuously rinsed with distilled water. Then, the polished electrode was allowed to dry in the air at room temperature.

The deposition (polymerization) of the cytosine monomer on the surface of the polished glassy carbon electrode was done by scanning in different potential windows between −1.2 and 1.8 V at a scan rate of 100 mVs^{-1} for 15 cycles in the 1.0 mM of cytosine.

The prepared poly(cytosine)/GCE was then washed by rinsing with distilled water many times to remove any nonreactive monomer from the electroactive surface of the electrode and stabilized in a monomer-free 0.5 M H_2SO_4 by scanning in the electrode potential window between 0.80 and −0.80 V until a steady cyclic voltammogram was obtained, and the new working electrode was assigned as poly(cytosine) modified glassy carbon electrode (poly(cytosine)/GCE). After the modified electrode was rinsed with distilled water, it was used for electrochemical studies.

2.2.4. Real Sample Preparation. 2.2.4.1. Human Blood Serum Sample. A leftover human blood sample was collected from Tibebe Ghion Hospital, Bahir Dar, Ethiopia, and stored in a refrigerator for 24 h. After that, 10 mL of the blood sample was then centrifuged at 4000 rpm for 15 min to remove all unwanted precipitating materials. The working solutions of serum samples for G determination were prepared by transferring 2.5 mL of the supernatant to 25 mL and filling it with ABS of pH 5 (1:10). Finally, spike recovery was investigated by preparing different concentrations of standard solutions of G spiked into the serum samples.

2.2.4.2. Human Urine Sample. A leftover human urine sample was collected from a Tibebe Ghion hospital at the laboratory level and centrifuged at a speed of 4000 rpm for 10 min. A 1 mL portion was transferred into a 25 mL flask and filled up to the mark with ABS of pH 5.0 solution. Various concentrations of G were prepared and spiked to the target samples for the recovery test.

2.2.4.3. DNA Extracts. DNA extract samples were collected from Bahir Dar University, biotechnology research laboratories. These extract samples were stored in the refrigerator until

https://doi.org/10.1021/acsomega.4c01939
ACS Omega 2024, 9, 26222−26234

investigation. The working solution of the DNA extracts was prepared by mixing with ABS at pH 5.0 in a ratio of 1:10.

3. RESULTS AND DISCUSSION

3.1. Fabrication of Poly(cytosine)/GCE. In the polymerization of cytosine on the surface of the electrode, the potential scan range was the most significant factor to be optimized, followed by the film thickness. No film was deposed on the surface of the electrode at potential windows narrower than −1.2 to +1.8 V. Hence, the optimized potential window for the cyclic voltammetric electropolymerization of cytosine at GCE was between −1.2 and +1.8 V, at a scan rate of 100 mVs^{-1} for 15 cycles of acetate buffer solution containing 1.0 mM of cytosine.

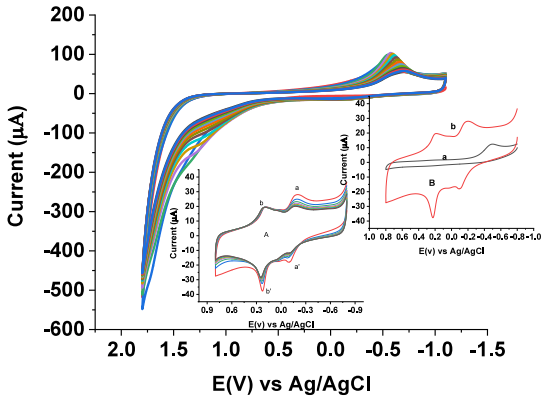

Figure 1. CVs of 1.0 mM cytosine scanned in the potential range of −1.2 to +1.8 V for 15 cycles at a 100 mVs^{-1} scan rate. Inset A: Cyclic voltammograms of (a) bare GCE and (b) poly(cytosine) of 0.5 H_2SO_4 in pH 5.0 ABS scanned between 0.8 and +0.8 V at 100 mV s^{-1}, Inset B: 8th cycle of H_2SO_4 stabilization of bare (a) and poly(cytosine)/GCE.

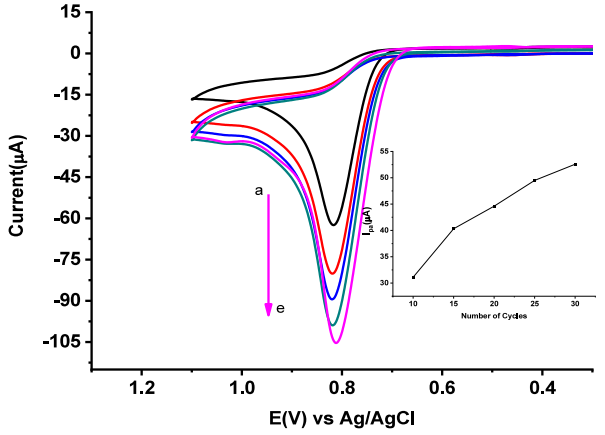

Figure 2. Blank corrected cyclic voltammograms of 1.0 mM G in pH 7.0 PBS at poly(cytosine)/GCE after different numbers of polymerization cycles (a−e: 10, 15, 20, 25, and 30, respectively) at 100 mVs^{-1}.

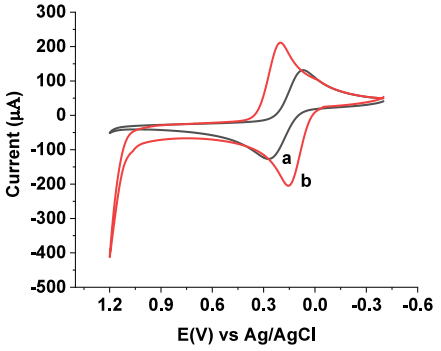

Figure 3. Cyclic voltammograms of (a) unmodified GCE and (b) poly(cytosine)/GCE modified GCE in 0.1 M KCl containing 10.0 mM $(Fe(CN)_6)^{3-/4-}$ in 0.1 M KCl at a scan rate of 100 mV s^{-1}.

During the electropolymerization of the cytosine monomer, a visible reductive peak at about −0.54 V, whose peak current increased with scan number, was seen (Figure 1). The current appearance is an indication of the electrodeposition of an electroactive polymer film on the GCE surface which is ascribed to the characteristic peak for the cytosine polymer film deposition through reduction-induced polymerization and consequently of the radical formation in between the ring and amide nitrogen within the cytosine.[20]

As can be realized from the voltammograms of bare GCE (inset curve A of Figure 1) and poly(cytosine)/GCE (inset curve B of Figure 1) in a monomer-free 0.5 M H_2SO_4 solution (inset A of Figure 1), a couple of two distinct redox peaks (a−a′) at about −0.03 and −0.02 V only at the poly(cytosine)/GCE indicated the successful deposition of a redox-active poly(cytosine) film at the surface of sensor GCE. In contrast to the electrochemically modified GCE, the only cathodic peak signal (of curve A) that emerged at the unmodified GCE around about −0.48 V was ascribed to molecular oxygen reduction, as shown in Figure 1, inset (A).

3.2. Optimization of Film Thickness. The number of cycles of the monomer (thickness of the film) adsorbed on the electroactive surface of GCE by electrochemical deposition is one of the useful pieces of information that affects the electrocatalytic performance of the electrode toward the analytes. Hence, the optimum film formed upon the variable number of cycles of monomer deposition on the modification process of the working GCE should be determined. The contribution of film thickness to the performance of the GCE was optimized by studying electrodepositing the cytosine monomer on the surface of the electrode with a varied number of CV cycles (10, 15, 20, 25, and 30 cycles), as depicted in Figure S1.

Initially, from 10 to 15 cycles, the anodic oxidative peak current of 1.0 mM G increased drastically, which might be due to a consecutive increase in the surface area of an electrode as thickness increases as a result of successive depositions of the monomer on the surface of the electrode. As the thickness of the polycytosine film increased beyond 15 cycles, the peak current of G started at a constant rate, which could be due to the surface hindrance of a high quantity of the film on the effective electroactive surface area of the electrode due to the overloading of the modifier on the electroactive surface that clogs the active surface of the electrode.[21]

Furthermore, the symmetric shape and oxidation peaks were recorded at lower oxidative potential by 15 cycles, which signifies the effective formation of an optimum sensing film at the electroactive surface of GCE. As can be seen clearly in the inset of Figure 2, starting from those points of view, a 15 cyclic electropolymerization potential scan was chosen as the optimal film thickness for fabricating Poly(cytosine)/GCE from its starting monomer material for the quantitative investigation of G in selected samples from clinical and body fluid samples.

3.3. Characterization of the Fabricated Poly-(cytosine)-Modified GCE. The electrochemical activity,

https://doi.org/10.1021/acsomega.4c01939
ACS Omega 2024, 9, 26222−26234

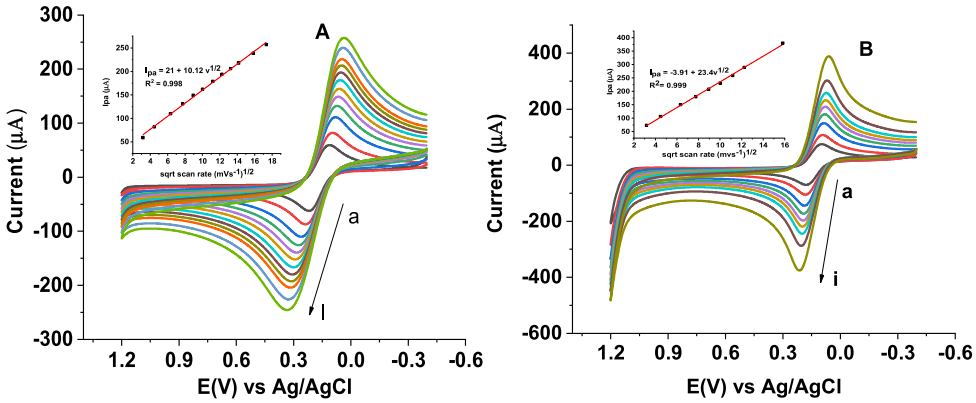

Figure 4. CVs of bare GCE (A) and poly(cytosine)/GCE (B) in 0.1 M KCl containing 10.0 mM $Fe(CN)_6^{3-/4-}$ in 0.1 M KCl at various scan rates (a–l: 10, 20, 40, 60, 80, 125, 150, 175, 200, 250, and 300 mVs^{-1}, respectively). Inset: a respective sketch of oxidative peak current versus square root of scan rate for both bare and poly(cytosine)/GCE.

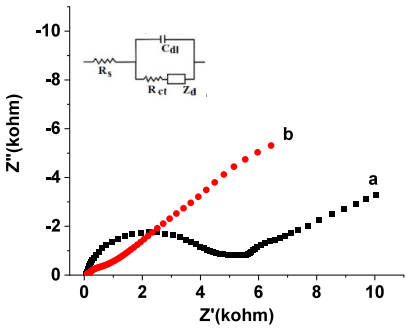

Figure 5. Nyquist plot of (b) bare GCE, (a) poly(cytosine)/GCE containing 10.0 mM $[Fe(CN)_6]^{3-/4-}$ and 0.1 M KCl inset: circuit diagram of the impedance.

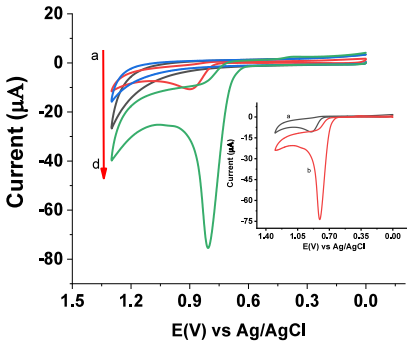

Figure 6. Cyclic voltammograms in the absence (a) and presence of 1 mM Guanine (c) at GCE, and the absence (b) and presence of 1 mM Guanine (d) at poly(cytosine)/GCE in pH 5.0 ABS at a scan rate of 100 mVs^{-1}. (inset: background corrected 1 mM Guanine on (a) GCE and (b) poly(cytosine)/GCE).

including electroactive surface area, electric current conduction, charge-transfer kinetics, and catalytic features of the developed biosensor, was characterized electrochemically using CV and EIS.

3.3.1. Cyclic Voltammetric Characterization. The electrochemical activity of poly(cytosine)/GCE was characterized by CV using $[Fe(CN)_6]^{3-/4-}$ as a redox probe as presented in Figure 3. The CV response of the poly(cytosine)/GCE is shown in Figure 3 for bare GCE (curve a) and poly(cytosine)/GCE (curve b) for 10.0 mM $[Fe(CN)_6]^{3-/4-}$ probe in a 0.1 M KCl at 100 mVs^{-1} of scan rates. A pair of reduction and oxidation peaks appearing on both bare and poly(cytosine)/GCE are ascribed to a one-electron electrochemical process of $[Fe(CN)_6]^{3-/4-}$. The ΔE_p was 228 mV for the unmodified GCE, and the poly(cytosine)/GCE showed improved electrocatalytic behavior with peak-to-peak potential separation (ΔE_p) of 50 mV. The formation of the enhanced peak current of the probe with narrower peak-to-peak separation at the poly(cytosine)/GCE might be due to an increased effective surface area of the electrode and improved charge transfer capability of the polymer film, indicating the electrocatalytic activity of the nobel modifier material.

As can be revealed from Figure 3, the redox peak potential difference at the unmodified GCE to the poly(cytosine)/GCE and peak current improvement at the poly(cytosine)-modified electrode by about 170% (1.7-fold) of the current response at the unmodified is clear verification for the successful deposition by electropolymerization of the monomer on the electroactive surface of the GCE.

To confirm the improvement of the active surface of the poly(cytosine)/GCE, the electroactive area of both the bare and poly(cytosine)/GCE was investigated. The influence of scan rate on the CV response of the bare and poly(cytosine)-based GCEs for $[Fe(CN)_6]^{3-/4-}$ as shown in Figure 4, was utilized for the determination of the effective electroactive surface area employing Randles-Sevcik equation (eq 1).[22,23]

$$I_p = 2.69 \times 10^5 AD^{1/2} n^{3/2} Cv^{1/2} \quad (1)$$

where I_P = peak current (amperes), n = stands for the number of electrons transferred in a redox cycle, A = the electrode surface area (cm^2), C = molar concentration of redox-active

Table 1. Summarized Circuit Parameters of the EIS Study

electrode	R_s (Ωcm^2)	R_{ct} (Ω cm^2)	frequency (Hz)	C_{dl} (F)	k^o
bare GCE	100	5140	251.18	1.23×10^{-7}	4.30×10^{-9}
poly(cytosine)/GCE	100	500	31.62	1.0×10^{-5}	4.40×10^{-8}

https://doi.org/10.1021/acsomega.4c01939
ACS Omega 2024, 9, 26222−26234

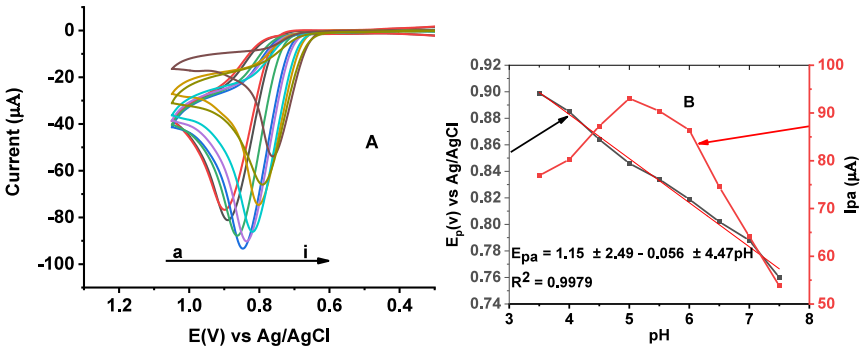

Figure 7. (A) CVs of poly(cytosine)/GCE in ABS of variable pH values (a−i: 3.5, 4.0, 4.5, 5.0, 5.5, 6.0, 6.5, 7.0, and 7.5, respectively) containing 1.0 mM G (B) plot of (a) peak potential and (b) peak current vs. pHs in the range of the pHs.

Scheme 1. Proposed Irreversible Oxidative Reaction Mechanism for G

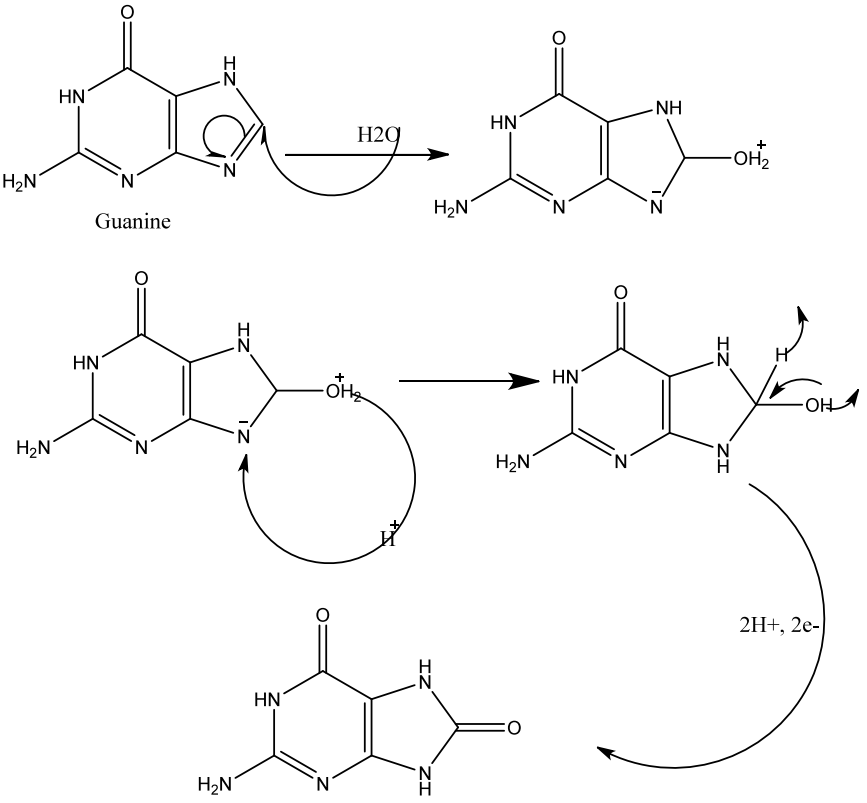

species (mol/cm^3), D = the diffusion coefficient (cm^2/s), and v = scan rate in V s^{-1}

Taking n = 1 for $[Fe(CN)_6]^{3-/4-}$ because 1 electron is being transferred during the redox process diffusion coefficient, D = 7.6 × 10^{-6} cm^2/s for $[Fe(CN)_6]^{3-/4-}$, the electroactive surface area calculated from the slope of the plot of anodic peak current versus square root of scan rate (inset of Figure 4A,B) was 0.136 cm^2 for unmodified GCE and 0.316 cm^2 for poly(cytosine)/GCE, showing that modification of the working electrode increased the effective surface area of the electrode by about 2.312 folds. The observed electrocatalytic effect of the modified surface toward current enhancement of $[Fe(CN)_6]^{3-/4-}$ was thus because of the increased electrode surface area.

3.3.2. Electrochemical Impedance Spectroscopic Characterization. EIS is utilized to characterize the charge transfer catalysis of the electrodes comparatively.[24] EIS was utilized to investigate an electrode's interface electrochemical properties. In comparison to the unmodified glassy carbon electrode (Figure 5, curve a), the poly(cytosine)/GCE (Figure 5, curve b) possessed a semicircle with a very small diameter, which is an indication that the surface of the electrode is modified with an electrochemically active polymer film that effectively activates the charge transfer conductivity of the electroactive surface. At poly(cytosine)/GCE, the charge-transfer resistance (R_{ct}) value, which is defined as the rate of charge exchange on the electrode−solution interface, decreased, implying the immobilization of highly conductive polymeric material with a high surface area that acted as electron transfer channels. Interestingly, poly(cytosine)/GCE exhibited a very low rate of charge-transfer resistance (high charge transfer) and high

https://doi.org/10.1021/acsomega.4c01939
ACS Omega 2024, 9, 26222−26234

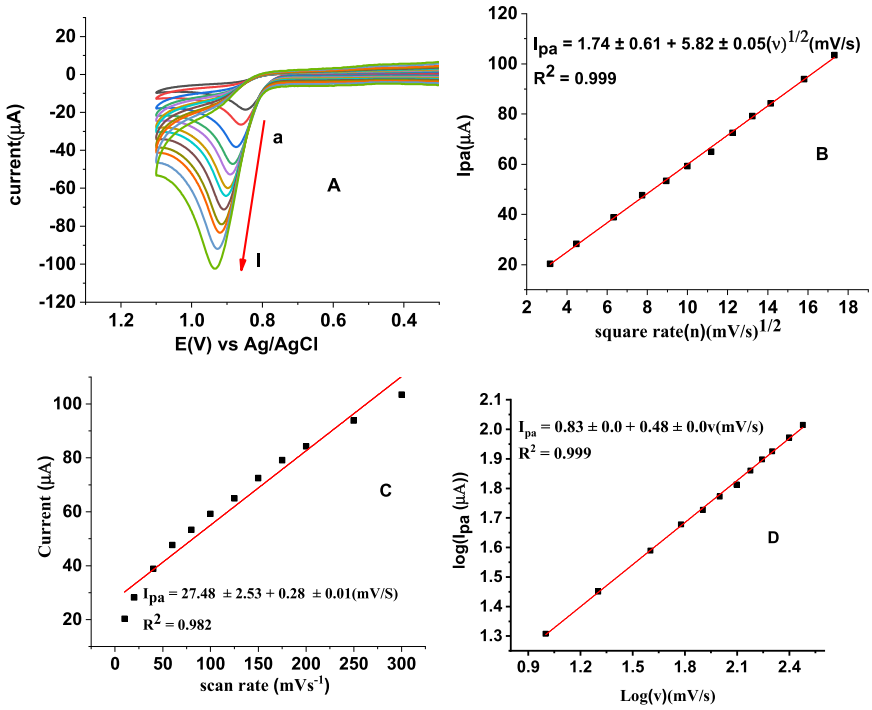

Figure 8. (A) CVs of poly(cytosine)/GCE in pH 5.0 ABS containing 1.0 mM G at various scan rates (a–l: 10, 20, 40, 60, 80, 100, 125, 150, 175, 200, 250, and 300 mVs^{-1}, respectively), (B) plot of I_p vs. $(v)^{1/2}$, (C) plot of I_p vs. scan rate, and (D) plot of log I_p vs. log (v).

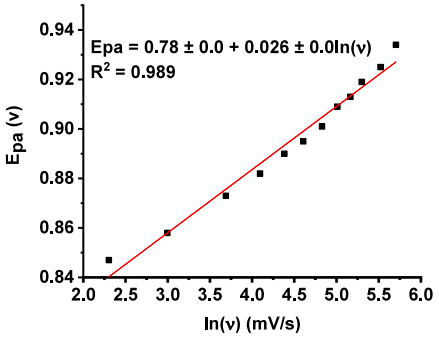

Figure 9. Plot of E_{pa} vs ln(scan rate) for 1.0 mM G at pH 5.0 of ABS on poly(cytosine)/GCE.

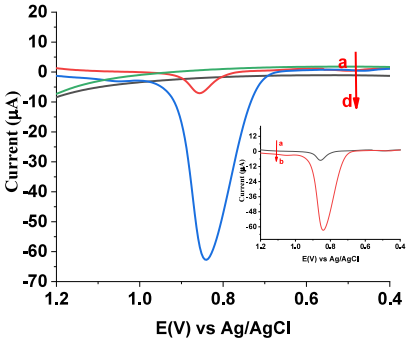

Figure 10. SWVs of unmodified GCE (a,c) and poly(cytosine)/GCE (b,d) at pH 5.0 ABS in the absence of G (a,b) and containing 1.0 mM G (c,d) at step potential: 4 mV, amplitude: 15 mV, and frequency of 25 Hz Inset: background subtracted SWVs of (a) bare GCE and (b) poly(cytosine)/GCE.

double-layer capacitance as compared to the unmodified electrode.

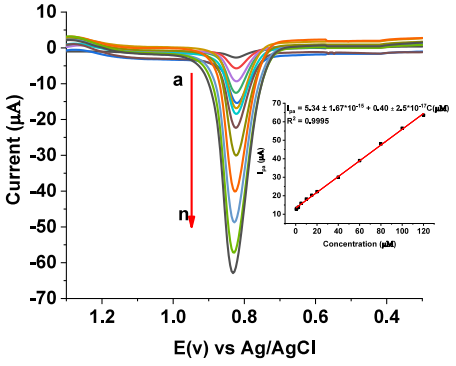

Figure 11. Blank corrected SWVs of poly(cytosine)/GCE in pH 5.0 ABS for varied concentrations of G (a–k: 0.1, 0.5, 1.0, 5.0, 10.0, 20.0, 40.0, 60.0, 80.0, 120, 160, and 200.0 μM, respectively) at a step potential of 4 mV, amplitude of 25 mV, and frequency of 25 Hz. Inset: plot of peak current vs. concentration of G.

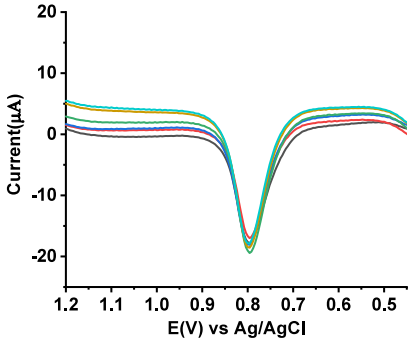

Figure 12. Blank corrected SWVs of poly(cytosine)/GCE in pH 5.0 ABS for intraday stability of 40 μM G at a stepping potential of 4 mV, amplitude of 25 mV, and SWV frequency of 25 Hz.

https://doi.org/10.1021/acsomega.4c01939
ACS Omega 2024, 9, 26222–26234

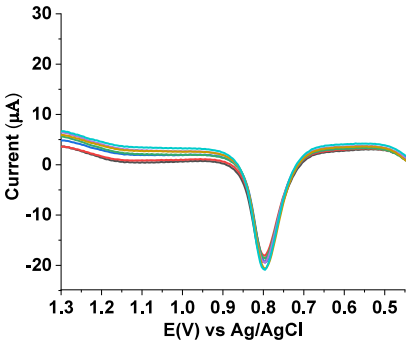

Figure 13. Blank corrected SWVs of poly(cytosine)/GCE in pH 5.0 ABS for intraday stability of 40 μM G at a stepping potential of 4 mV, amplitude of 25 mV, and SWV frequency of 25 Hz.

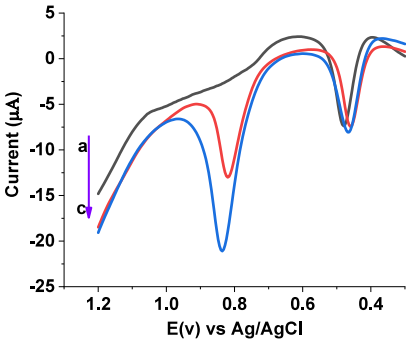

Figure 14. Background subtracted SWVs of poly(cytosine)/GCE in pH 5.0 ABS containing (a) unspiked urine sample, (b) + 20.0 μM standard G, and (c) + 40.0 μM standard G. at a stepping potential of 4 mV, square wave amplitude of 25 mV, and pulse frequency of 25 Hz.

Table 2. Recovery Study of Various Concentrations of G in Spiked Urine, Serum, and DNA Samples

sample	added standard (μM)	expected (μM)	found (μM)[a]	recovery
	0.0	0.0	0.0	0.0
urine	20.0	20.0	19.86 ± 2.10	99.30
	40.0	40.0	39.65 ± 1.70	99.13
	0.0	0.0	0.0	0.0
serum	20.0	20.0	19.65 ± 2.34	98.25
	40.0	40.0	40.06 ± 1.76	100.15
	0.0	0.00	1.40 ± 1.21	
DNA	20.0	21.40	22.25 ± 0.83	103.97%
	40.0	41.40	41.28 ± 1.52	99.71%

[a]Mean ± %RSD for n = 3.

From Figure 5, it can be observed that both the surface untreated (bare) GCE and poly(cytosine)/GCE revealed semicircles of different diameters at the high-frequency region and a line at about 45° at the low-frequency region attributed to diffusion of the probe from the bulk solution toward the site of the electrode−solution interface.[25] From the Nyquist plot, the diameter of the semicircle at a higher frequency region resembles the charge-transfer resistance (R_{ct}) of the current electrode, and the linear portion at the lower frequency region represents the diffusion process.[25] The R_{ct} value of poly-(cytosine)/GCE, which is (500 Ω) much less than bare GCE (5140 Ω), is an indication of a higher diffusion rate of the electron due to the surface activation of GCE that is agreed

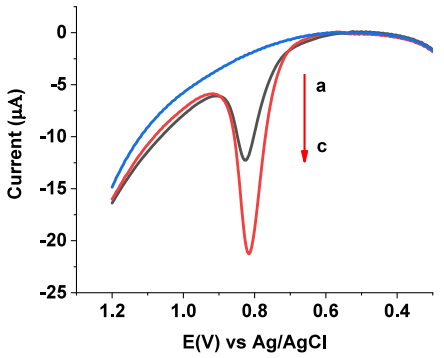

Figure 15. Background subtracted SW voltammograms of poly-(cytosine)/GCE in pH 5.0 ABS containing (a) unspiked blood serum sample, (b) serum sample +20.0 μM standard G, and (c) serum sample +40.0 μM standard G. at a stepping potential of 4 mV, SWV amplitude of 25 mV, and SWV frequency of 25 Hz.

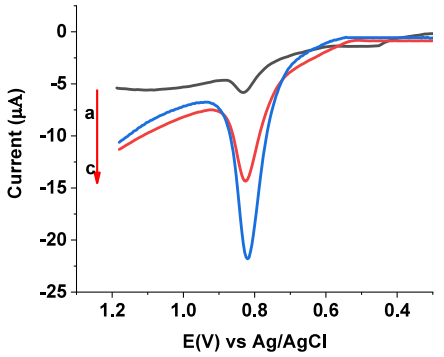

Figure 16. Background subtracted SW voltammograms of poly-(cytosine)/GCE in pH 5.0 ABS containing (a) unspiked blood serum sample, (b) serum sample +20.0 μM standard G, and (c) serum sample +40.0 μM standard G at a step potential of 4 mV, amplitude of 25 mV, and SWV frequency of 25 Hz.

Table 3. Summary of Interference Recovery Results of G Containing Concentrations: 20.0−120.0 μM DIC, GA, and UA

interferent	interferent added (μM)	current response (μA)	expected current (μA)	recovery	% error
	0	20.08			
	20	19.98	20.08	99.50	0.5
UA	40	20.54	20.08	102.30	2.3
	80	20.60	20.08	102.58	2.58
	120	20.71	20.08	103.10	3.1
	0	20.08			
	20	19.88	20.08	99.00	0.99
GA	40	19.89	20.08	99.05	0.95
	80	20.02	20.08	99.70	0.30
	120	20.28	20.08	100.99	0.99
	0	20.08	20.08		
	20	20.51	20.08	102.14	2.14
DIC	40	20.89	20.08	104.03	4.03
	80	21.28	20.08	105.97	5.97
	120	21.45	20.08	106.82	6.82

with those resulted from the CV characterization of the current study. This result reveals the successful deposition of the ploy(cytosine) at the GCE surface. The double layer capacity of the GCE (C_{dl}) and charge transfer rate (k^o) for both bare

https://doi.org/10.1021/acsomega.4c01939
ACS Omega 2024, 9, 26222−26234

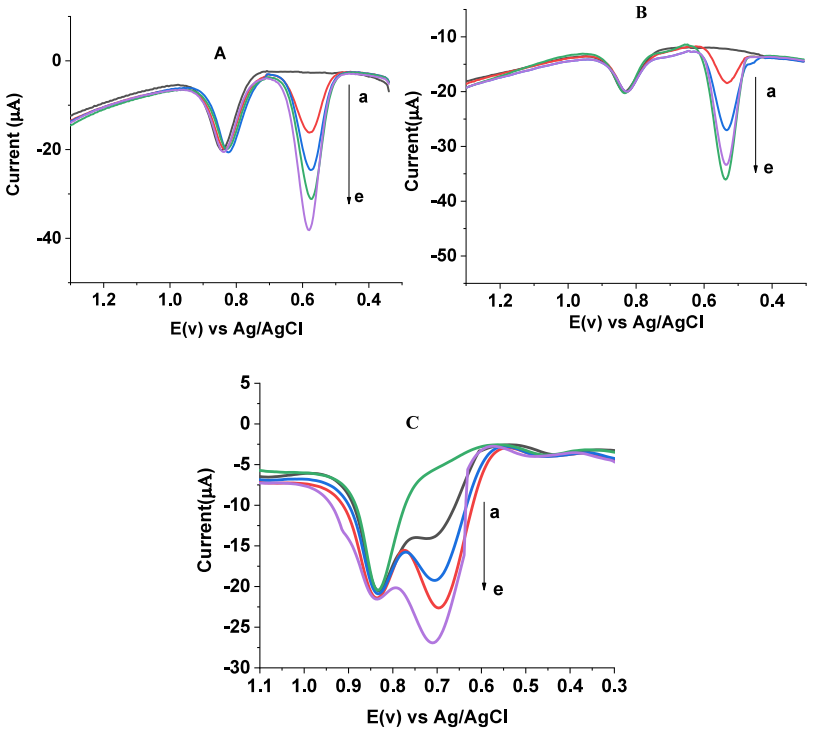

Figure 17. Background cs of 40.0 μM G standard solution (pH5.0 ABS) containing different concentrations of interfering substances (A) gallic acid, (B) uric acid, (C) diclofenac, at concentrations a−e: 0.0, 20.0, 40.0, 80.0, and 120.0 μM) at a stepping potential of 4 mV, amplitude of 25 mV, and SWV frequency of 25 Hz.

Table 4. Summary of Comparison of the Figures of Merits of the New Sensor with the Reported Methods

modifier	electrode	technique	LOD (μM)	linear range (μM)	refs
NF/CHT-ARGO	NF/CHT-ARGO/GCE	DPV	0.10	0.10−120	41
GMC	GMC/GCE	DPV	0.76	25−150	42
$Au_{50}Pt_{50}$NCs-rGO	$Au_{50}Pt_{50}$NCs-rGO/GCE	SWV	0.06	1−200	43
GS/IL/CHT	GS/IL/CHT/GCE	DPV	0.75	2.5−150	44
graphene-NF	graphene-NF/GCE	DPV	0.58	10−300	45
PANI/MnO_2	PANI/MnO_2/GCE	DPV	4.80	10−100	46
SWCNT-Lys	SWCNT-Lys/GCE	LSV	0.075	0.2−25	47
MWCNT/CHT	MWCNT/CHT/GCE	DPV	0.06	0.2−450	48
PPDA/CRGO	PPDA/CRGO/GCE	DPV	0.01	0.05−6.00	49
poly(cytosine)	poly(cytosine)/GCE	SWV	0.0061	0.1−200	this work

and poly(cytosine)/GCE are computed by applying the equations as portrayed below (eq 2) and (eq 3), respectively, and summarized clearly in Table 1.

$$C_{dl} = \frac{1}{2\pi R_{ct} f_{max}} \quad (2)$$

where C_{dl} is the double-layer capacitance, R_{ct} is the charge-transfer resistance of the interface double layer, and f_{max} is the frequency corresponding to the maximum imaginary impedance on the Nyquist plot diagram.

Conversely, from the Nyquist plot of the EIS analysis, the rate of charge transfer (k^o) at the GCE and poly(cytosine)/GCE is obtained byeq 3:

$$k^o = \frac{RT}{n^2F^2ACR_{ct}} \quad (3)$$

where k^o is the charge transfer rate, R is the universal gas constant, T is the Kelvin temperature, A is the electroactive area, and others as usual.

3.4. Study of the Electrochemical Behavior of G on Poly(cytosine)/GCE. The electrochemical feature of G on cyclic voltammetric investigation at poly(cytosine)/GCE was performed by analysis of 1 mM G and compared with that of the unmodified GCE (Figure 6). As can be depicted from Figure 6, the appearance of a single well-resolved oxidative peak at around 800 mV potential in both bare and poly(cytosine)/GCE, and no peak in the backward scan direction for G is an indication of the irreversible oxidation of G at both unmodified and poly(cytosine)/GCE. The observed oxidative peak current response at the poly(cytosine)/GCE (curve b of inset of Figure 6) is around 7.5-fold (over 65 μA) to the oxidative peak signal at the unmodified GCE (curve b of inset of Figure 6). This could be ascribed to the high surface roughness and effective area of the polymer-modified electrode.

In addition to that, the anodic peak potential of G at the poly(cytosine)/GCE appearing at less potential than (E_p = 800 mV) that of the bare GCE (E_p = 893 mV) is supposed to

https://doi.org/10.1021/acsomega.4c01939
ACS Omega 2024, 9, 26222−26234

improve the charge transfer capability of the poly(cytosine)/GCE.

Generally speaking, after surface modification, the improvement of the oxidative peak current response of G and its peak-to-peak potential reduction at poly(cytosine)/GCE is an indication of the electrocatalytic ability of the complex modifier toward the electrooxidation of G.

The potential decrease by about 93 mV is confirmed by the modifier's electrocatalytic activity for G oxidation, and a 7.5-fold peak current augmentation may have caused the reported increases in conductivity and surface area.

3.5. Investigation of Effect of Electrolytic Solutions. The kind of buffer solution also has an impact on the electrochemical activity of an electroactive species. The most used types of supporting electrolytes having high buffering capacities are acetate buffer solution (ABS), Britton-Robinson buffer solution (BRBS), and phosphate buffer solution (PBS) [86]. Figure S2 displays the cyclic voltammetric signals of 1 mM G at pH 5.0 of different buffer solutions. As can be shown in Figure S2, a highly intensive oxidative peak at a lower electrode potential, with an enhanced peak current for G in the modified electrode, is obtained in ABS.

3.6. pH Effect on Peak Current and Peak Potential. Investigating the effect of the pH of the supporting electrolytic solution on the current response and peak potential direction of an electroactive species at an electrode is one piece of information that helps us study the involvement of proton and electron in the redox reaction. Figure 7 explains the influence of pH on the oxidation peak current and potential of 1.0 mM G in ABS using poly(cytosine)/GCE in ABS. As observed from Figure 7, the anodic peak potential shifts toward the negative direction as pH varies from 3.5 to 7.5 (Figure 7A), which confirms the participation of the proton in the electrochemical oxidation reaction of G on the surface of poly(cytosine)/GCE. From the plot of oxidation peak potential versus pH (Figure 7B), the slope of 0.056 V (curve (a)) indicates the involvement of electrons and protons in a 1:1 ratio,[26] and the proposed reaction scheme for the oxidation route of G is represented in reaction Scheme 1 below.

On the other hand, the oxidative peak current of G at the poly(cytosine)/GCE increased with pH values increasing from 3.5 to 5.0 (curve (b) of Figure 7B) after then decreasing at pH regions beyond 5.0 (curve (b) of Figure 7B), which may be attributable to the interaction of the G with the electrode-modifying materials. G presents a pK_a value of 4.2, and the increasing current trend in the acidic region might account partly for the possible attraction between guanine and the cytosine (pK_a 9.2) deposited by electropolymerization in the reduced form.[27,28]

3.7. Effect of Scan Rate on I_{pa} and E_{Pa} of G Oxidation. One parameter that determines the behavior of the analyte's response, the rate that determines the step, and the participation of protons and electrons is the scan rate. The influence of scan rate on the signal form of peak current signal and the position peak potential of G at poly(cytosine)/GCE was investigated, as shown in Figure 8. As can be perceived from Figure 8, the observed oxidation peak potential of G shifts to a more positive direction with an increase in the scan rate (Figure 8A). The potential shift upon scan rate strongly indicates that the electrochemical oxidation of G is irreversible. Then again, from the linear correlation curve, a higher correlation (R^2 = 0.999) for the dependence of peak current on the square root of scan rate (Figure 8B) than on scan rate (R^2 = 0.982) (Figure 8C) is an indication that the electrochemical oxidation of G at poly(cytosine)/GCE was predominantly a diffusion-controlled process.[29] That was also confirmed by the slope of 0.48 for the plot of the logarithmic value of peak current versus logarithmic scan rate, which nearly agrees with the ideal value of 0.5 for the diffusion-controlled process (Figure 8D).[30−32]

In addition, the number of participant electrons that incorporated/involved in the electroanalytical behavior of the G oxidation at poly(cytosine)/GCE was determined from the response of CV by taking a sole scan rate simply by determining the αn values from the irreversible process. This was calculated by taking the difference between the peak potential (E_p) and the half-wave potential ($E_{p1/2}$) usingeq 4:[33]

$$E_p - E_{p1/2} = \frac{47.7}{\alpha n} \tag{4}$$

where α stands for the charge transfer coefficient, and n implies the number of electrons participated. At the scan rate of 100 mVs^{-1}, the peak potential E_p and halve wave potential $E_{p1/2}$ values for the CV of G (from scan rate) are obtained to be 908 and 861 mV, respectively, and the value of αn was calculated and obtained as 1.01. Considering α for an irreversible electrode−solution interaction process is 0.50,[30] the number of electrons (n) transferred in the electroanalytical oxidation of G at the active surface of poly(cytosine)/GCE was estimated at 2.03 (~2.0).

For the irreversible electrochemical reactions, the relation between E_p and ln(v) obeys eq 5.

$$E_p = E^{O} + \frac{RT}{(1-\alpha)nF}\left\{0.780 + \ln\left(\frac{D_R^{1/2}}{k^o}\right) + \ln\left[\frac{(1-\alpha)nFv}{RT}\right]^{1/2}\right\} \tag{5}$$

where E_p = peak potential, E^o = the forma potential, α = the electron transfer coefficient, k^o = the electrochemical rate constant, R is the universal gas constant, F is Faraday's constant, T is Kelvin temperature, and the other parameters with their usual meanings.

From the plot of E_{pa} versus ln v (Figure 9), taking the slope of 0.026 (slope = $\frac{RT}{(1-\alpha)nF}$ = 0.026 for the fitted line ($E_{pa}(v)$ = 0.78 + 0.026 ln (v) of the curve of the plot of E_{pa} versus ln(v).

At laboratory room temperature (approximately 25 °C) and taking n = 2 for G oxidation, the value of (1 − α) was calculated using eq 3 and obtained to be 0.5. Taking the one electron for the oxidation of G calculated using eq 4, the coefficient of electron transfer (α) was found to be 0.5, confirming the irreversibility of the electroanalytical oxidation of G.[34]

3.8. Quantitative Investigation of G at Poly(cytosine)/GCE by SWV. For quantitative monitoring of G in clinical and biological matrixes, square wave voltammetry was applied because, with its maximum sensitivity and very low detection limit, it is the most effective electroanalytical technique for quickly decaying the nonfaradic current.[35] Figure 10 shows the square wave voltammograms of with and without 1 mM G in pH 5.0 ABS at unmodified and poly(cytosine)/GCE and voltammogram of background corrected bare (curve of inset a) and poly(cytosine)/GCE (curve of inset b). As depicted in Figure 10, the appearance of well-shaped and highly intensive

https://doi.org/10.1021/acsomega.4c01939
ACS Omega 2024, 9, 26222−26234

oxidate square wave voltammograms with about 9-fold current performance improvements was noticed. This confirms the contribution of the poly(cytosine) as the catalytic activator for the electrooxidation of G toward poly(cytosine)/GCE.

3.9. Optimization of the SWV Parameters. For further analysis, selected SWV parameters (step potential, pulse amplitude, and wave frequency) were optimized. Although an increase in peak current response with an increase in step potential, frequency, and square wave amplitude is implicit, these parameters should be investigated and optimized by agreeing with the response of the increased Faradaic peak current and complemented capacitive current.

3.9.1. Effect of Step Potential. The oxidative peak current of 1.0 mM G at the poly(cytosine)/GCE increased with step potential in the range from 2 to 12 mV (Figure S3). However, the increase in oxidative peak current is accompanied by a loss of peak symmetry range and peak potential shift. Additionally, the peak current increment decreases at high step potentials. Thus, a step potential of 4 mV was chosen as the optimum step potential for further square wave voltammetric analysis due to the drastically enhanced Faradaic current.

3.9.2. Effect of Square Wave Amplitude. The effect of square wave amplitude on the oxidative peak current of G at the poly(cytosine)/GCE was checked in the wave amplitude range of 10−45 mV (Figure S4). A square wave amplitude of 25 mV was chosen as a compromise between the peak current increment and the accompanied peak broadening.

3.9.3. Effect of Frequency. The influence of SW voltammetric frequency on the current intensity of G on poly(cytosine)/GCE was studied, and the result is depicted in Figure S5. The response of the electrode toward G at various frequencies reveals the increase in the intensity of the peak current with frequencies, which is similar to the trend observed for the effect of amplitude. A frequency value of 25 Hz was chosen for reasons similar to those for the stepping potential and pulse amplitude.

3.10. Calibration Curve and Detection Limit of the Developed Method. Under optimized experimental conditions and parameters, the SWV responses of varying concentrations (between 0.1 and 200 μM) were investigated (Figure 11). The limit of detection and limit of quantification were calculated by LOD = 3 s/m and LOQ = 10 s/m[36,37] where s is the standard deviation of the blank for quintuplicate measurements and m is the slope of the calibration curve. By utilizing the formula, LOD and LOQ were found to be 6.1 and 20.13 nM, respectively (inset of Figure 11). Associated %RSD values were under 1% for triplicate measurement, showing the precision of the developed novel electrochemical biosensor based on the poly(cytosine) as an electrode modifier.

3.11. Stability and Reproducibility Studies. To investigate the long-term stability, accuracy, and repeatability developed a biosensor for selective and reproducible measurements, the performances of the modified electrodes were evaluated by recording six successive SWVs of the developed electrochemical sensor in pH 5.0 ABS containing 40.0 μM G at an interval of 2 hrs. in a day as shown in Figure 12 with an error of 3% (%RSD). This indicates the qualitative effectiveness of the proposed sensor for successive applications in biological samples.

Similarly, the long-term stability and repeatability developed G biosensor for selective and reproducible measurements of 40.0 μM G at pH 5.0 ABS were studied for 14 successive days with SWVs at an interval of 2 days between days as presented in Figure 13 with a relative error (%RSD) of 3.4%. This result also confirms that the valuable activity of the proposed sensor is the best alternative means for reproducible material for electrochemical determination of G from different samples and is highly stable for repeatable response for sensor application.

3.12. Application of Poly(cytosine)/GCE for Determination of G in Real Sample. The valuable application of the current biosensor was confirmed by applying it in real sample analysis. The due sensor was used to successfully determine the G from clinical blood serum, urine, and laboratory-level extracted DNA samples.

3.12.1. Human Urine Sample. Figure 14 represents SW voltammograms for a clinical human urine leftover sample prepared following the procedure described elsewhere in the experimental procedure.[38] It can be clearly understood from Figure 14 that the voltammetric signal without any significant peak at the characteristic potential of G indicates that the urine sample does not contain active G in the analyzed human urine sample (Figure 14 peak A), and the appearance of a sharp peak intensity at a potential away from the characteristic potential for G is attributed for the existence of potentially active uric acid in the urine sample (peak B of Figure 14).[39,40] The selectivity of the newly proposed method for quantification of G in human urine by adding a certain quantity of uric acid was further examined by a spike recovery test. The spike recovery investigation was studied by adding 20 and 40 μM standard solutions of G into a urine sample and is enclosed in Table 2. The spike recovery of the proposed material on G determination from the urine sample was in the range of 99.13 to 99.30%, indicating the robust applicability of the sensor for quantitative determination and qualitative diagnostic analysis.

3.12.2. Human Blood Serum Sample. For further application, the validity of the developed biosensor was utilized for the analysis of G from leftover blood serum samples collected from the hospital. Figure 15 shows background subtracted SWV for a human blood serum sample prepared by following the procedure explained in the procedure part elsewhere. Without any considerable quantity of standard G, there was no observable signal of a peak current at the characteristic potential of G, indicating the absence of the target analyte in the analyzed human serum sample, while after the addition of a known concentration of G, the corresponding peak intensity enhancement was observed (peaks b and c of Figure 15) [140, 141]. The selectivity of the developed method for G in human serum was further examined by a spike recovery test. The recovery test was computed from the spiked standards, and the recovery results were obtained in the range of 98.25 to 100.15% (Table 2).

3.12.3. DNA Extract Samples. Furthermore, the applicability of the current electrochemical poly(cytosine)/GCE-based sensor for the screening and determination of G was investigated from DNA samples extracted from human blood samples. This was done by determining the target analyte from DNA extract without and with spiking a known concentration of standard G. As presented in Figure 16, there is the appearance of peak current (peak a) for the detected G in the unspiked DNA, and there is an increase of current response intensity with the increase of the concentration of spiked standard G, indicating that the peak was because of the existence of G in DNA.

The spike recovery of results of G in the collected DNA extract sample was obtained in the percentage between 99.71

https://doi.org/10.1021/acsomega.4c01939
ACS Omega 2024, 9, 26222−26234

and 103.97% as shown in Table 2 with %RSD under 3.7% for G in the human DNA sample validated the novel electrochemical sensor for successful determination of G in the human DNA sample.

3.13. Interference Study. For the valid application, during the G determination, different samples such as serum, DNA, and urine samples containing some potential interferents were investigated successfully. In this study, the compounds that are expected to be potential interferents, such as uric acid and gallic acid, were evaluated. The outcome of the added-on intensity peak current of the analyte is outlined in Table 3.

The contribution of each interferent was investigated at a variable concentration of those potential interferents, as can be seen in Figure 17. As the quantity of the interferences varies, their peak current varies accordingly; conversely, there is no change in the oxidative peak current response of the G, indicating the developed sensor is highly selective toward the targeted species.

Table 3 shows the concentration of G detected as the concentration of the spiked interferents varied. In all the cases, G was recovered between 97.86 and 103.10%. This confirms that the studied interferents could not affect the determination of G, and hence that the developed electrochemical biosensor was valid for the study of G from real samples in the presence of interfering compounds.

3.14. Comparison of the Present Work with the Reported Methods. The performance characteristics of the present sensor electrode, such as the type of modifier, linear range of detection, detection limit, availability of the electrode modifier, and cost, were compared with some of the recently reported voltammetric methods for the study of the oxidation of G, as depicted in Table 4.

The present poly(cytosine)/GCE manifested a very wide linear range and the lowest LOD value of all of the previously reported works. Thus, the current reported method based on poly(cytosine) film from an easily accessible cytosine monomer as a modifier showed a supercilious performance over those that used expensive electrode modifiers.

4. CONCLUSIONS

Poly(cytosine)-based biosensor was developed for the detection of Guanine (G), and characterization of the sensor was done by CV and EIS. The electrochemical behavior of G at the poly(cytosine)/GCE was studied through CV. Moreover, the study of the dependency of peak current on the square root of the scan rate pointed toward a diffusion-controlled process of G at poly(cytosine)/GCE. Notably, the shift in peak potential with pH highlighted proton involvement in the electrochemical oxidation of G.

For the sensitive and selective determination of G in different samples like blood serum, urine, and DNA extracts, SWV based on poly(cytosine)/GCE was employed and revealed a linear relationship between the oxidative peak response and G concentration within the range of 0.1−200 μM, with an impressive limit of detection and limit of quantification of 6.10 and 20.13 nM, respectively.

Real sample analysis confirmed that only DNA extracts contained detectable G, measuring around 1.40 μM, which falls below the permissible level of G in human blood DNA. The sensor was assessed for interference, stability, and reproducibility, affirming its reliability for quantitative and qualitative G analysis. In conclusion, the newly developed sensor proved to be highly sensitive, selective, and stable, demonstrating its efficacy for G detection and analysis.

■ ASSOCIATED CONTENT

Supporting Information

The Supporting Information is available free of charge at https://pubs.acs.org/doi/10.1021/acsomega.4c01939.

CV of 1.0 mM Cytosine at 10, 15, 20, 25, and 30 cycles; CV response of poly(cytosine)/GCE of 1 mM Guanine in various electrolytes; SWVs of poly(cytosine)/GCE for 1 mM Guanine at different step potentials; SWVs of poly(cytosine)/GCE for 1 mM Guanine at different pulse amplitudes; and SWVs of poly(cytosine)/GCE for 1 mM Guanine at different frequencies (PDF)

■ AUTHOR INFORMATION

Corresponding Author

Melaku Metto − *Department of Chemistry, College of Science, Bahir Dar University, Bahir Dar 6000, Ethiopia; Department of Chemistry, College of Natural and Computational Sciences, Injibara University, Injibara 6400, Ethiopia;* orcid.org/0000-0001-8291-3185; Email: melakumetto@gmail.com

Authors

Alemu Tesfaye − *Department of Chemistry, College of Science, Bahir Dar University, Bahir Dar 6000, Ethiopia*

Minaleshewa Atlabachew − *Department of Chemistry, College of Science, Bahir Dar University, Bahir Dar 6000, Ethiopia*

Atakilt Abebe − *Department of Chemistry, College of Science, Bahir Dar University, Bahir Dar 6000, Ethiopia;* orcid.org/0000-0002-5496-664X

Tihunie Fentahun − *Department of Chemistry, College of Science, Bahir Dar University, Bahir Dar 6000, Ethiopia*

Abaineh Munshea − *Department of Chemistry, College of Science, Bahir Dar University, Bahir Dar 6000, Ethiopia*

Complete contact information is available at: https://pubs.acs.org/10.1021/acsomega.4c01939

Author Contributions

A.A. conceptualized the research. A.M. was involved in the extraction of DNA samples. M.M. collected samples, designed and conducted the experiment, analyzed and interpreted the result, and drafted and wrote the script. A.T., M.A., and A.A. supervised the work, interpreted the result, and edited the script. T.F. contributed to data collection and assisted with the laboratory analysis. All authors read and approved the final manuscript.

Notes

The authors declare no competing financial interest.
The authors have agreed to the publication of this work upon its acceptance.

■ ACKNOWLEDGMENTS

Melaku Metto Ambo is thankful to Injibara University for sponsoring his PhD study. We greatly acknowledge the Swedish International Development Cooperation Agency (SIDA) through the International Science Programme, Uppsala University (ISP) for their financial support.

REFERENCES

(1) Shantharaja; Nemakal, M.; Giddaerappa; Gopal Hegde, S.; Koodlur Sannegowda, L. Novel biocompatible amide phthalocyanine for simultaneous electrochemical detection of adenine and guanine. *Microchem. J.* **2022**, *175*, No. 107223.

(2) Shantharaja; Nemakal, M.; Giddaerappa; Koodlur Sannegowda, L. Biocompatible polymeric pyrazolopyrimidinium cobalt(II) phthalocyanine: An efficient electroanalytical platform for the detection of l-arginine. *Sensors and Actuators A: Physical* **2021**, *324*, No. 112690.

(3) Mirica, A. C.; Stan, D.; Chelcea, I. C.; Mihailescu, C. M.; Ofiteru, A.; Bocancia-Mateescu, L. A. Latest Trends in Lateral Flow Immunoassay (LFIA) Detection Labels and Conjugation Process. *Front Bioeng Biotechnol* **2022**, *10*, No. 922772.

(4) Ren, Q. L.; Wang, Q.; Zhang, X. Q.; Wang, M.; Hu, H.; Tang, J. J.; Yang, X. T.; Ran, Y. H.; Liu, H. H.; Song, Z. X.; et al. Anticancer Activity of Diosgenin and Its Molecular Mechanism. *Chin J. Integr. Med.* **2023**, *29*, 738−749.

(5) Ibrahim, H.; Temerk, Y.; Farhan, N. Electrochemical sensor for individual and simultaneous determination of guanine and adenine in biological fluids and in DNA based on a nano-In−ceria modified glassy carbon paste electrode. *RSC Adv.* **2016**, *6* (93), 90220−90231.

(6) Badralmaa, Y.; Natarajan, V. Impact of the DNA extraction method on 2-LTR DNA circle recovery from HIV-1 infected cells. *J. Virol Methods* **2013**, *193* (1), 184−189.

(7) Yan, X.; Shu, Q.; Zhao, K.; Xiao, Y.; Ai, F.; Zheng, X. Chemiluminescence "signal-on-off" dual signals ratio biosensor based on single-stranded DNA functions as guy wires to detect EcoR V. *Talanta* **2021**, *235*, No. 122749.

(8) Brohi, R. O. Z. Z.; Khuhawar, M. Y.; Khuhawar, T. M. J. GC-FID determination of nucleobases guanine, adenine, cytosine, and thymine from DNA by precolumn derivatization with isobutyl chloroformate. *Journal of Analytical Science and Technology* **2016**, *7* (1), 10.

(9) Zhou, Y.; Yan, H.; Xie, Q.; Yao, S. Determination of guanine and adenine by high-performance liquid chromatography with a self-fabricated wall-jet/thin-layer electrochemical detector at a glassy carbon electrode. *Talanta* **2015**, *134C*, 354−359.

(10) Wang, W.; Zhou, L.; Wang, S.; Luo, Z.; Hu, Z. Rapid and simple determination of adenine and guanine in DNA extract by micellar electrokinetic chromatography with indirect laser-induced fluorescence detection. *Talanta* **2008**, *74* (4), 1050−1055.

(11) Zhang, J.-X.; Lv, C.-L.; Tang, C.; Wang, A.-J.; Mei, L.-P.; Song, P.; Feng, J.-J. Sandwich-type ultrasensitive immunosensing of breast cancer biomarker based on core-shell Au@PdAg dog-bone-like nanostructures and Au@PtRh nanorods. *Sensors Actuators B: Chem.* **2023**, *382*, No. 133497.

(12) Yang, L.; Wang, A.-J.; Weng, X.; Feng, J.-J. Well-dispersed strawberry-like PtCo nanocrystals/porous N-doped carbon nanospheres for multiplexed assays. *Microchem. J.* **2023**, *187*, No. 108421.

(13) Balasubramanian, P.; Settu, R.; Chen, S.-M.; Chen, T.-W. Voltammetric sensing of sulfamethoxazole using a glassy carbon electrode modified with a graphitic carbon nitride and zinc oxide nanocomposite. *Microchimica Acta* **2018**, *185* (8), 396.

(14) Yang, L.; Zhu, Y.-P.; Wang, A.-J.; Weng, X.; Feng, J.-J. Simple pyrolysis of graphene-wrapped PtNi nanoparticles supported on hierarchically N-doped porous carbon for sensitive detection of carbendazim. *Microchimica Acta* **2023**, *190* (6), 211.

(15) Švorc, Ľ.; Kalcher, K. Modification-free electrochemical approach for sensitive monitoring of purine DNA bases: Simultaneous determination of guanine and adenine in biological samples using boron-doped diamond electrode. *Sens. Actuators, B* **2014**, *194*, 332−342.

(16) Xu, J.; Li, T.; Shen, S.; Zhao, L.; Ma, C.; Abdelaal, M.; Wang, J. Electrochemically Reduced Carboxyl Graphene Modified Electrode for Simultaneous Determination of Guanine and Adenine. *Anal. Lett.* **2015**, *48*, 1465.

(17) Papavasileiou, A. V.; Trachioti, M. G.; Hrbac, J.; Prodromidis, M. I. Simultaneous determination of guanine and adenine in human saliva with graphite sparked screen-printed electrodes. *Talanta* **2022**, *239*, No. 123119.

(18) Zhang, S.; Zhuang, X.; Chen, D.; Luan, F.; He, T.; Tian, C.; Chen, L. Simultaneous voltammetric determination of guanine and adenine using MnO2 nanosheets and ionic liquid-functionalized graphene combined with a permeation-selective polydopamine membrane. *Microchimica Acta* **2019**, *186* (7), 450.

(19) Hua, Y.; Li, S.; Cai, Y.; Liu, H.; Wan, Y.; Yin, M.; Wang, F.; Wang, H. A sensitive and selective electroanalysis strategy for histidine using the wettable well electrodes modified with graphene quantum dot-scaffolded melamine and copper nanocomposites. *Nanoscale* **2019**, *11* (5), 2126−2130.

(20) Wang, Y.; Zhao, H.; Yang, C.; Jie, J.; Dai, X.; Zhou, Q.; Liu, K.; Song, D.; Su, H. Degradation of Cytosine Radical Cations in 2′-Deoxycytidine and in i-Motif DNA: Hydrogen-Bonding Guided Pathways. *J. Am. Chem. Soc.* **2019**, *141* (5), 1970−1979.

(21) Elugoke, S. E.; Fayemi, O. E.; Adekunle, A. S.; Sherif, E.-S. M.; Ebenso, E. E. Electrochemical sensor for the detection of adrenaline at poly(crystal violet) modified electrode: optimization and voltammetric studies. *Heliyon* **2022**, *8* (10), No. e10835.

(22) Gira, M. J.; Tkacz, K. P.; Hampton, J. R. Physical and electrochemical area determination of electrodeposited Ni, Co, and NiCo thin films. *Nano Converg* **2016**, *3* (1), 6.

(23) Wagnew, A.; Kassa, A.; Abebe, A.; Asmellash, T.; Beyene, Y.; Tesfaye, A.; Amare, M. Poly(aquachlorobis(1,10−phenanthroline)-copper(II)iodidemonohydrate)/GCE for simultaneous determination of caffeine and theophylline in human serum, tea, and tablet samples. *Arabian Journal of Chemistry* **2022**, *15* (1), No. 103458.

(24) Amiri, M.; Imanzadeh, H.; Sefid-Sefidehkhan, Y. An Overview on Electrochemical Sensors Based on Nanomaterials for the Determination of Drugs of Abuse. *Curr. Drug Delivery* **2021**, *18* (2), 162−183.

(25) Iurilli, P.; Brivio, C.; Wood, V. On the use of electrochemical impedance spectroscopy to characterize and model the aging phenomena of lithium-ion batteries: a critical review. *J. Power Sources* **2021**, *505*, No. 229860.

(26) Kumar, N.; Rosy; Goyal, R. N. Gold-palladium nanoparticles aided electrochemically reduced graphene oxide sensor for the simultaneous estimation of lomefloxacin and amoxicillin. *Sens. Actuators, B* **2017**, *243*, 658−668.

(27) Pollap, A.; Knihnicki, P.; Kuśtrowski, P.; Kozak, J.; Gołda-Cępa, M.; Kotarba, A.; Kochana, J. Sensitive Voltammetric Amoxicillin Sensor Based on TiO2 Sol Modified by CMK-3-type Mesoporous Carbon and Gold Ganoparticles. *Electroanalysis* **2018**, *30* (10), 2386−2396.

(28) Quiroz-Arturo, H.; Reinoso, C.; Scherf, U.; Palma-Cando, A. Microporous Polymer-Modified Glassy Carbon Electrodes for the Electrochemical Detection of Metronidazole: Experimental and Theoretical Insights. *Nanomaterials* **2024**, *14*, 180.

(29) Kassa, A.; Bitew, Z.; et al. A non-toxic poly(resorcinol) modified glassy carbon electrode for highly Selective Square wave voltammetry determination of aspirin in tablet formulations and human urine samples. *Sens. Bio-Sens. Res.* **2023**, *39*, No. 100554.

(30) Nigussie, M.; Kassa, A.; Guadie, A.; Mulu, M.; Lijalem, T.; Tefera, M. Selective and sensitive determination of tinidazole in pharmaceuticals and biological matrix using poly(diphenylamine −4-sulfonic acid) modified glassy carbon electrode. *Sensing and Bio-Sensing Research* **2023**, *39*, No. 100552.

(31) Jesny, S.; Girish Kumar, K. Non-enzymatic Electrochemical Sensor for the Simultaneous Determination of Xanthine, its Methyl Derivatives Theophylline and Caffeine as well as its Metabolite Uric Acid. *Electroanalysis* **2017**, *29* (7), 1828−1837.

(32) Antakli, S.; Nejem, L.; Ahmad, W. A. Determination of Amoxicillin Trihydrate by Analytical Spectrophotometry. *Research Journal of Pharmacy and Technology* **2019**, *12* (6), 2716−2720.

(33) Kassa, A.; Abebe, A.; Amare, M. Synthesis, characterization, and electropolymerization of a novel Cu(II) complex based on 1,10-phenanthroline for electrochemical determination of amoxicillin in pharmaceutical tablet formulations. *Electrochim. Acta* **2021**, *384*, No. 138402.

https://doi.org/10.1021/acsomega.4c01939
ACS Omega 2024, 9, 26222−26234

(34) Bard, A. J.; Faulkner, L. R.; White, H. S. *Electrochemical methods: fundamentals and applications*; John Wiley & Sons: 2022.
(35) López-Tenés, M.; Laborda, E.; Martínez-Ortiz, F.; González, J.; Molina, A. Square wave voltammetry as a powerful tool for studying multi-electron molecular catalysts. *J. Electroanal. Chem.* **2022**, *927*, No. 116943.
(36) Zoubir, J.; Radaa, C.; Idlahcen, A.; Bakas, I.; Assabbane, A. A new voltammetric sensor for metronidazole based on electro catalytic effect of Al2O3 modified carbon graphite. Application. Urine, tap water and river water. *Materials Science for Energy Technologies* **2021**, *4*, 296−306.
(37) Alemu, T.; Zelalem, B.; Amare, N. Voltammetric Determination of Ascorbic Acid Content in Cabbage Using Anthraquinone Modified Carbon Paste Electrode. *J. Chem.* **2022**, *2022*, No. 7154170.
(38) Kassa, A.; Amare, M. Highly selective and sensitive differential pulse voltammetric method based on poly(Alizarin)/GCE for determination of cefadroxil in tablet and human urine samples. *Arabian Journal of Chemistry* **2021**, *14* (8), No. 103296.
(39) Tefera, M.; Tessema, M.; Admassie, S.; Wubet, W. Voltammetric determination of uric acid using multiwall carbon nanotubes coated-poly(4-amino-3-hydroxy naphthalene sulfonic acid) modified glassy carbon electrode. *Heliyon* **2021**, *7* (7), No. e07575.
(40) Metto, M.; Eramias, S.; Gelagay, B.; Washe, A. P. Voltammetric Determination of Uric Acid in Clinical Serum Samples Using DMF Modified Screen Printed Carbon Electrodes. *Int. J. Electrochem.* **2019**, *2019*, No. 6318515.
(41) Li, D.; Yang, X.-L.; Xiao, B.-L.; Geng, F.-Y.; Hong, J.; Sheibani, N.; Moosavi-Movahedi, A. A. Detection of Guanine and Adenine Using an Aminated Reduced Graphene Oxide Functional Membrane-Modified Glassy Carbon Electrode. *Sensors* **2017**, *17* (7), 1652.
(42) Thangaraj, R.; Senthil Kumar, A. Simultaneous detection of guanine and adenine in DNA and meat samples using graphitized mesoporous carbon modified electrode. *J. Solid State Electrochem.* **2013**, *17* (3), 583−590.
(43) Mao, B.; Qian, L.; Govindhan, M.; Liu, Z.; Chen, A. Simultaneous electrochemical detection of guanine and adenine using reduced graphene oxide decorated with AuPt nanoclusters. *Microchimica Acta* **2021**, *188* (8), 276.
(44) Niu, X.; Yang, W.; Ren, J.; Guo, H.; Long, S.; Chen, J.; Gao, J. Electrochemical behaviors and simultaneous determination of guanine and adenine based on graphene−ionic liquid−chitosan composite film modified glassy carbon electrode. *Electrochim. Acta* **2012**, *80*, 346−353.
(45) Yin, H.; Zhou, Y.; Ma, Q.; Ai, S.; Ju, P.; Zhu, L.; Lu, L. Electrochemical oxidation behavior of guanine and adenine on graphene−Nafion composite film modified glassy carbon electrode and the simultaneous determination. *Process Biochemistry* **2010**, *45* (10), 1707−1712.
(46) Anu Prathap, M. U.; Srivastava, R.; Satpati, B. Simultaneous detection of guanine, adenine, thymine, and cytosine at polyaniline/MnO2 modified electrode. *Electrochim. Acta* **2013**, *114*, 285−295.
(47) Gutiérrez, A.; Gutierrez, F. A.; Eguílaz, M.; González-Domínguez, J. M.; Hernández-Ferrer, J.; Ansón-Casaos, A.; Martínez, M. T.; Rivas, G. A. Electrochemical sensing of guanine, adenine and 8-hydroxy-2′-deoxyguanosine at glassy carbon modified with single-walled carbon nanotubes covalently functionalized with lysine. *RSC Adv.* **2016**, *6* (16), 13469−13477.
(48) Wang, P.; Wu, H.; Dai, Z.; Zou, X. Simultaneous detection of guanine, adenine, thymine and cytosine at choline monolayer supported multiwalled carbon nanotubes film. *Biosens. Bioelectron.* **2011**, *26* (7), 3339−3345.
(49) Li, C.; Qiu, X.; Ling, Y. Electrocatalytic oxidation and the simultaneous determination of guanine and adenine on (2,6-pyridinedicarboxylic acid)/graphene composite film modified electrode. *J. Electroanal. Chem.* **2013**, *704*, 44−49.

https://doi.org/10.1021/acsomega.4c01939
ACS Omega 2024, 9, 26222−26234